AMERICAN SOCIETY FOR MICROBIOLOGY | Journal of Virology

A Haploid Genetic Screen Identifies Heparan Sulfate Proteoglycans Supporting Rift Valley Fever Virus Infection

Amber M. Riblett,[a] Vincent A. Blomen,[b] Lucas T. Jae,[b] Louis A. Altamura,[c] Robert W. Doms,[d] Thijn R. Brummelkamp,[b,e] Jason A. Wojcechowskyj[a]*

Department of Microbiology, Perelman School of Medicine, University of Pennsylvania, Philadelphia, Pennsylvania, USA[a]; Netherlands Cancer Institute, Amsterdam, The Netherlands[b]; Diagnostic Systems Division, United States Army Medical Research Institute of Infectious Diseases, Fort Detrick, Maryland, USA[c]; Department of Pathology and Laboratory Medicine, Children's Hospital of Philadelphia, Philadelphia, Pennsylvania, USA[d]; Cancer Genomics Center, Utrecht, The Netherlands[e]

ABSTRACT

Rift Valley fever virus (RVFV) causes recurrent insect-borne epizootics throughout the African continent, and infection of humans can lead to a lethal hemorrhagic fever syndrome. Deep mutagenesis of haploid human cells was used to identify host factors required for RVFV infection. This screen identified a suite of enzymes involved in glycosaminoglycan (GAG) biogenesis and transport, including several components of the *cis*-oligomeric Golgi (COG) complex, one of the central components of Golgi complex trafficking. In addition, disruption of *PTAR1* led to RVFV resistance as well as reduced heparan sulfate surface levels, consistent with recent observations that PTAR1-deficient cells exhibit altered Golgi complex morphology and glycosylation defects. A variety of biochemical and genetic approaches were utilized to show that both pathogenic and attenuated RVFV strains require GAGs for efficient infection on some, but not all, cell types, with the block to infection being at the level of virion attachment. Examination of other members of the *Bunyaviridae* family for GAG-dependent infection suggested that the interaction with GAGs is not universal among bunyaviruses, indicating that these viruses, as well as RVFV on certain cell types, employ additional unidentified virion attachment factors and/or receptors.

IMPORTANCE

Rift Valley fever virus (RVFV) is an emerging pathogen that can cause severe disease in humans and animals. Epizootics among livestock populations lead to high mortality rates and can be economically devastating. Human epidemics of Rift Valley fever, often initiated by contact with infected animals, are characterized by a febrile disease that sometimes leads to encephalitis or hemorrhagic fever. The global burden of the pathogen is increasing because it has recently disseminated beyond Africa, which is of particular concern because the virus can be transmitted by widely distributed mosquito species. There are no FDA-licensed vaccines or antiviral agents with activity against RVFV, and details of its life cycle and interaction with host cells are not well characterized. We used the power of genetic screening in human cells and found that RVFV utilizes glycosaminoglycans to attach to host cells. This furthers our understanding of the virus and informs the development of antiviral therapeutics.

Rift Valley fever virus (RVFV) is a member of the *Bunyaviridae* family of viruses that cause emerging infections that threaten both human and livestock populations on several continents (1). Bunyaviruses have a tripartite, negative-sense RNA genome and are frequently transmitted by insects (1). RVFV can be transmitted by mosquitoes or by exposure to infected tissues and body fluids and is considered endemic in much of Africa (2). In humans, RVFV can cause an acute fever leading to complications such as kidney failure and, in about 1% of cases, a lethal hemorrhagic fever (3, 4). In addition, RVFV spreads rapidly across infected herds of livestock and can cause significant mortality in infected animals (5, 6).

We took a genetic approach to identify host factors that are required for RVFV infection *in vitro* by employing an insertional mutagenesis screen using HapI cells, a human haploid cell line. By utilizing a retroviral gene trap, gene-inactivating insertion sites can be efficiently mapped with deep sequencing technology (7). This approach has successfully uncovered host factors required by a variety of pathogens, including viruses, bacteria, and bacterial toxins (8–12). When gene trap-mutagenized HapI cells were challenged with RVFV and the surviving cells were analyzed, there was an enrichment of sites of insertion into multiple genes involved in glycosaminoglycan (GAG) biosynthesis as well as genes for subunits of the *cis*-oligomeric Golgi (COG) complex and *PTAR1*. We confirmed the requirement for heparan sulfate during infection with RVFV isolates with a variety of genetic and biochemical perturbations, consistent with the findings from de Boer et al. (13). We now show that the dependency on heparan sulfate during

Received 13 August 2015 **Accepted** 10 November 2015

Accepted manuscript posted online 18 November 2015

Citation Riblett AM, Blomen VA, Jae LT, Altamura LA, Doms RW, Brummelkamp TR, Wojcechowskyj JA. 2016. A haploid genetic screen identifies heparan sulfate proteoglycans supporting Rift Valley fever virus infection. J Virol 90:1414–1423. doi:10.1128/JVI.02055-15.

Editor: T. S. Dermody

Address correspondence to Jason A. Wojcechowskyj, Jason.Wojcechowskyj@ucsf.edu.

* Present address: Jason A. Wojcechowskyj, Gladstone Institutes, San Francisco, California, USA, and University of California, San Francisco, San Francisco, California, USA.

A.M.R., V.A.B., and L.T.J. contributed equally to this article.

RVFV infection is consistent across a representative panel of primary RVFV isolates and, by employing vesicular stomatitis virus (VSV)-based pseudovirions, that utilization of GAGs by RVFV during infection occurs at the step of entry. We were able to identify, using a quantitative binding assay, virus attachment to be the specific entry step affected. However, the dependence of RVFV on GAGs for efficient infection was cell type dependent. Surfen (a small-molecule antagonist of heparan sulfate) inhibited infection of HapI and SNB-19 cells by replication-competent RVFV, yet surfen did not impact infection of several other cell lines by RVFV, even though it efficiently blocked infection by herpes simplex virus 1 (HSV-1), a virus that depends upon heparan sulfate for efficient infection *in vitro*. Thus, while GAG interactions do significantly enhance RVFV infection in some contexts, other virus attachment factors must also exist and/or RVFV utilizes GAG structures that do not efficiently interact with surfen.

MATERIALS AND METHODS

Cells and viruses. HapI cells (7) and the derived mutant cell lines were grown in Iscove's modified Dulbecco's medium (IMDM) supplemented with 10% (vol/vol) fetal bovine serum (FBS), 2 mM L-glutamine, 1 mM sodium pyruvate, 10 units/ml penicillin, and 100 μg/ml streptomycin. HEK 293T, Vero E6, C6/36, L, and sog9 cells (a generous gift from Frank Tufaro) were grown in Dulbecco's modified Eagle medium (DMEM) supplemented with 10% (vol/vol) FBS, 2 mM L-glutamine, 10 units/ml penicillin, and 100 μg/ml streptomycin.

The following strains of RVFV were used in this study: MP-12, ZH-501, Kenya 9800523, and Kenya 2007002444. MP-12 was propagated in MRC-5 cells (at the University of Pennsylvania) or Vero E6 cells (at USAMRIID), while the ZH-501 and the Kenyan strains were propagated in Vero E6 cells. Viral titers on Vero E6 cells were determined by plaque assay. Crimean-Congo hemorrhagic fever virus (CCHFV) strain IbAr10200 was propagated in CER cells, and viral titers on CER cells were determined. HSV-1 strain k-GFP (a generous gift from Nigel Fraser, University of Pennsylvania) was propagated in Vero E6 cells. Studies using RVFV ZH-501 were conducted in a biosafety level 3 laboratory at USAMRIID, whereas infections using the Kenyan RVFV strains and CCHFV were performed in a biosafety level 4 laboratory at USAMRIID. Appropriate safety protocols were followed, and personal protective equipment was worn while conducting experiments in the high-containment laboratories. The generation of PTAR1-deficient HapI cells was described before (14).

Insertional mutagenesis. HapI cells were mutagenized with a retroviral gene trap as described in reference 11 and exposed to strain MP-12. Surviving clones were expanded for genomic DNA isolation. Subsequently, gene trap insertion sites were amplified using an inverse PCR, submitted for parallel sequencing (Illumina HiSeq 2000), and aligned to the human genome (hg18) (10). Genes significantly enriched for gene-trap insertions compared to the sequences of an unselected control cell population were identified using a one-sided Fisher's exact test as described in reference 11.

RVFV pseudovirion production. To assess the specific role of GAGs in RVFV attachment and entry, as opposed to downstream replication events, we used a VSV pseudovirion system (15, 16) in which the VSV glycoprotein gene G was deleted from the viral genome (VSVΔG) and replaced with a reporter gene, either *Renilla* luciferase (VSVΔG-rLuc) or red fluorescent protein (VSVΔG-RFP). To generate VSVΔG pseudovirions possessing RVFV glycoproteins (or those of other viruses), the glycoproteins were provided in *trans* via an expression vector to cells transduced with the VSVΔG core. HEK 293T cells seeded in 10-cm^2 plates were transfected with pCAGGS RVFV ZH-548 M using the Lipofectamine 2000 reagent (Invitrogen) according to the manufacturer's instructions. This construct is codon optimized for expression in human cells and contains only the coding region of the M segment starting at the fourth ATG start codon, which omits the NS_M coding region. At between 16 and 20 h after transfection, cells were transduced with VSVΔG pseudovirions bearing VSV G. After adsorption of pseudovirions for 1 h, cells were carefully rinsed four times with warm phosphate-buffered saline (PBS) containing calcium and magnesium, and then the medium was replaced with complete DMEM supplemented with 25 mM HEPES. Cell culture supernatants were collected 24 h later, clarified by low-speed centrifugation for 30 min at 4°C, filtered (pore size, 0.45 μm), and then aliquoted for storage at −80°C. Andes virus (ANDV) and Hantaan virus (HTNV) pseudovirions were generated in the same fashion.

Virus infections. To compare the ability of diverse RVFV strains or CCHFV to infect HapI cells and the derived mutant cell lines, we utilized a high-content imaging-based infection assay. Each cell line was seeded at a density of 1×10^4 cells per well in Greiner black well, clear-bottom 96-well plates. At 24 h after seeding of the cells, the culture medium was removed and the cells were infected with viruses diluted in complete IMDM. The virus inocula were not washed off and the plates were incubated at 37°C until approximately 18 to 20 h postinfection. At this point, the cell culture medium was removed from the cells and the plates were immersed in 10% neutral buffered formalin for 24 h to fix the cells and render virus noninfectious prior to removal from the high-containment laboratories.

Prior to immunostaining for viral antigens, residual formalin was removed from the plates, and they were then rinsed extensively with phosphate-buffered saline (pH 7.4). The cells were permeabilized for 15 min with a solution of 0.1% (vol/vol) Triton X-100 in PBS, and then the permeabilization buffer was rinsed away by additional PBS washes. The cells were blocked for at least 1 h using a 3% (wt/vol) solution of bovine serum albumin in PBS. Purified monoclonal antibodies specific for RVFV N (R3-1D8) or CCHFV N (9D5-1-1A) were diluted 1:1,000 in blocking buffer and then added to the cells for 1 h, followed by extensive washing with PBS. Anti-mouse immunoglobulin Alexa Fluor 568-labeled secondary antibody was diluted 1:2,000 in blocking buffer and then added to the cells for 1 h, followed by extensive washing in PBS. The cells were then counterstained with a solution of Hoechst 33342 (nuclei) and HCS CellMask deep red stain (total cell), each of which was diluted 1:10,000 in PBS. This counterstain solution was maintained on the plates during high-content imaging.

Automated image acquisition was performed using an Operetta high-content imaging system. Three exposures (one for each of the fluorophores) in five separate fields were acquired in each well using a 20× air objective and a Peltier cooled 1.3-megapixel charge-coupled-device camera. The fluorophores were illuminated using a 300-W xenon arc light source and excitation (EX) and emission (EM) filters for the following: Alexa Fluor 568 (EX/EM), Hoechst 33342 (EX/EM), and HCS CellMask deep red (EX/EM). Image segmentation and analysis were performed using Harmony (version 3.0) software and standard scripts. These algorithms were used to first delineate nuclear and cell boundaries and then identify viral antigens by Alexa Fluor 568 staining. To calculate percent infection per image field, the number of cells exhibiting an Alexa Fluor 568 mean fluorescence intensity greater than the mean intensity for uninfected control wells was divided by the total cell number defined by Hoechst 33342 nuclear staining. For each well, the Harmony software reported the mean percent infection of the five fields. On average, 1,500 to 5,000 cells were analyzed per well. In each independent experiment, at least 4 individual wells were analyzed for each cell line.

Infections with VSVΔG-RFP pseudovirions or HSV-1 were carried out at a low volume for 1 h at 37°C, after which complete DMEM or IMDM was added to the wells. Twenty-four hours later, the cells were trypsinized, fixed in 2% paraformaldehyde and then analyzed for RFP (for VSVΔG pseudovirions) or green fluorescent protein (GFP) (for HSV-1) expression by fluorescence-activated cell sorting (FACSCalibur flow cytometer; BD Biosciences). For infections in the presence of surfen (5 μM; Sigma), dextran sulfate (5 μg/ml, 5 kDa; Sigma), or heparinase I (3 U/ml;

Sigma), cells were pretreated for 1 h and, in the case of surfen and dextran sulfate, kept in the presence of drug for the duration of the infection. For soluble GAG competition experiments, heparin (10 and 100 μg/ml; Fisher BioReagents) and heparan sulfate (10 and 100 μg/ml; Iduron) were preincubated with HSV-1 or MP-12 at 25°C for 1 h. The virus and GAG solution was then allowed to adsorb onto cells for 1 h at 37°C, after which it was rinsed 3 times with PBS containing calcium and magnesium and cells were refed with fresh medium that did not contain either virus or GAGs. Infections were then harvested at 8 to 10 h postinfection (hpi), and percent infection was scored by flow cytometry, looking for either intracellular staining of the N protein (for MP-12) or expression of the GFP reporter protein (for HSV-1). For pseudovirion neutralization studies, RVFV and severe acute respiratory syndrome (SARS) coronavirus antisera (a generous gift from Stuart Nichol, Centers for Disease Control and Prevention) were preincubated with pseudovirions at the indicated dilutions for 30 min at 37°C. The linear range of the assay was determined by performing serial 10-fold dilutions of each virus stock on each target cell type and for each detection method used. Infection assays were typically linear over at least a 2-log-unit range of virus dilutions, with the virus inoculum being adjusted to achieve infection levels of between 1 and 30%.

RVFV binding assay. Virus was diluted in DMEM (Gibco) and added to HapI cells and the derived mutant cell lines for 1 h at 37°C. The cells were then washed four times with PBS, and total RNA was isolated from the cells using a Qiagen RNeasy minikit. RNA was quantified by measuring the absorbance at 260 nm, and first-strand cDNA was generated from 1.5 μg of total RNA using a SuperScript VILO cDNA synthesis kit (Invitrogen) according to the manufacturer's instructions. Primers specific to the MP-12 L segment (forward L segment primer 5′-TGAGAATTCCTG AGACACATGG-3′; reverse L segment primer 5′-ACTTCCTTGCATCA TCTGATG-3′) were purchased from Invitrogen, and a 6-carboxyfluorescein/MGB probe specific to the MP-12 L segment with the sequence 5′-CAATGTAAGGGGCCTGTGTGGACTTGTG-3′ was purchased from Applied Biosystems. Reverse transcription-PCR (RT-PCR) was then performed using an ABI 7500 real-time PCR system (Applied Biosystems) with the following conditions: (i) denaturation at 95°C for 20 s and (ii) 40 cycles of PCR amplification with denaturation at 95°C for 3 s and annealing and extension at 60°C for 30 s. Data were analyzed using the $\Delta\Delta C_T$ threshold cycle (C_T) method by calculating the change in gene expression normalized to that of *GAPDH* (glyceraldehyde-3-phosphate dehydrogenase) as a housekeeping gene (17).

Statistical analysis. Statistical significance was calculated using a two-tailed, one-sample *t* test by comparing the fold changes to the hypothetical value of 1 in Prism software (version 5.0a; GraphPad Software). *P* values were not reported for conditions where only two biological replicates were performed.

RESULTS

An insertional mutagenesis screen for RVFV host factors in a human haploid cell line. To identify the host factors needed for RVFV infection, 1×10^8 HapI cells were mutagenized using a retroviral gene trap vector (11). Subsequently, mutagenized cells were infected with the cytotoxic RVFV MP-12 strain and the surviving cells were expanded as a polyclonal cell population. Following isolation of genomic DNA, gene trap insertion sites were sequenced and aligned to the human genome. Subsequently, the retroviral insertions within genes in the virus-resistant population were counted and compared to the number of insertions within the same gene in an unselected cell population (11). Genes significantly enriched ($P < 0.001$) for insertions in the virus-selected cell population were identified (Fig. 1A). These contain multiple genes encoding enzymes required for synthesis of glycosaminoglycans, including the four enzymes needed for the tetrasaccharide linkage region (XYLT2, B4GALT7, B3GAT3, and B3GALT6) (18–23), two enzymes involved in proteoglycan chain elongation (EXT1 and EXT2) (24), and the enzyme that catalyzes both N-deacetylation and N-sulfation during the biosynthesis of heparan sulfate (NDST1) (25). Genes required for the synthesis (*UXS1*, *UGDH*) or transport (*SLC35B2*) of critical moieties for heparan sulfate chain formation (26–28) were also enriched in cells resistant to RVFV infection (Fig. 1A and B). In addition to genes directly involved in heparan sulfate biosynthesis, several subunits of the conserved oligomeric Golgi (COG) complex (*COG1*, *COG2*, *COG3*, *COG4*, *COG5*, *COG7*, *COG8*) (29) were identified from the screen. It is known that perturbation of the COG complex attenuates O-linked glycosylation by impairing Golgi complex function (29, 30). Another hit in this screen encoded UNC50, a Golgi complex-resident transmembrane protein that plays a role in nicotinic acetylcholine receptor trafficking in *Caenorhabditis elegans* (31). Finally, this screen identified the gene for prenyltransferase alpha subunit repeat containing 1 (*PTAR1*) to be important for RVFV infection. PTAR1 was previously shown to affect glycosylation (11), possibly by influencing vesicular trafficking through prenylation of Rab GTPases (14, 32). Although genes involved in vesicular trafficking could represent more direct interactions with RVFV, the overlap of these results with those from a screen performed for cell surface GAG expression (11) suggests a function for these genes in the presentation of glycans at the cell surface.

GAGs are important for RVFV infection. Because the majority of genes identified in our screen pertained to GAG synthesis, we first focused on elucidating the role of GAGs during RVFV infection. We were able to obtain single-cell clones of gene-trapped *B3GAT3* (*B3GAT3*^{GT}) and *B4GALT7* (*B4GALT7*^{GT}) and exposed these cells to the MP-12 strain of RVFV. As shown in Fig. 2A, these cells were markedly resistant to MP-12 infection. Importantly, reintroduction of the respective cDNAs completely restored sensitivity to virus infection, indicating that the observed resistance phenotype can be solely attributed to the gene-trapped loci (Fig. 2A). To determine whether the synthesis of the O-linked tetrasaccharide linker was required for RVFV infection, we produced a *B3GAT3*^{GT} cell line stably expressing an enzymatically inactive point mutant of GlcAT-I (D194A/D195A) (33). As with the *B3GAT3*^{GT} cells stably expressing an empty vector construct, introduction of this enzymatically inactive form of GlcAT-I into *B3GAT3*^{GT} cells did not rescue MP-12 infection (Fig. 2B). *B4GALT7* encodes the β-1,4-galactosyltransferase GalT-I, which catalyzes the enzymatic step immediately upstream of the β-1,3-galactosyltransferase reaction in the synthesis of the GAG linker (Fig. 1B). As with the *B3GAT3*^{GT} cell panel, MP-12 infection also required a catalytically active form of GalT-I (Fig. 2B), further suggesting that RVFV is dependent upon GAGs for efficient infection.

For some viruses, the requirement for GAGs for infection of cells in culture is a trait acquired during *in vitro* passaging, often leading to attenuation (34–36). To determine whether this was the case with RVFV, we infected the *B3GAT3*^{GT} and *B4GALT7*^{GT} cell panels with three pathogenic strains of RVFV: ZH-501, Kenya 9800523 (1998), and Kenya 2007002444 (2007). We found that infection by these primary RVFV strains was also strongly inhibited in cells lacking functional GlcAT-I and GalT-I. Infection was rescued by expression of the wild-type construct but not the enzymatically inactive constructs (Fig. 2B). The dependence of primary RVFV strains upon these enzymes indicates that the require-

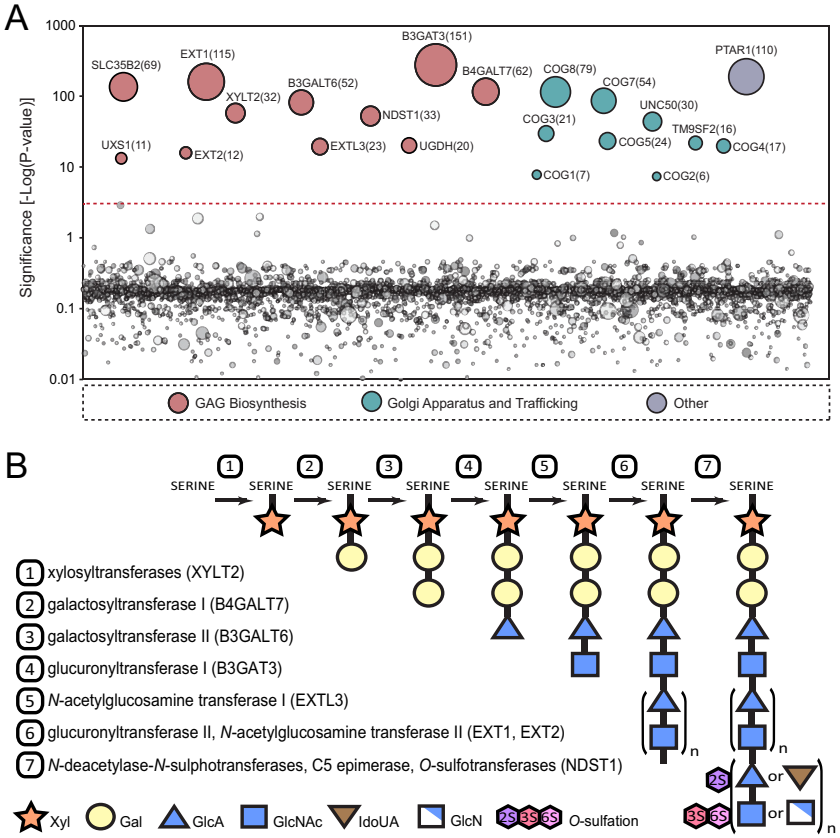

FIG 1 Human haploid mutagenesis screen for RVFV host factors. (A) Plot showing genes enriched in the virus-selected population compared with their levels in an unselected population. Each circle demarks a gene, with its *y*-axis coordinate representing the false discovery rate-corrected *P* value and its area reflecting the number of identified unique gene trap integrations. Genes that are significantly enriched in the virus-selected population ($P < 0.001$) are colored and horizontally grouped on the basis of their function. (B) Overview of heparan sulfate synthesis. Genes involved in heparan sulfate synthesis that were significantly enriched in our RVFV screen are shown in parentheses.

ment of GAGs for viral infection is not due to cell culture adaption or attenuation.

To further test the hypothesis that RVFV infection requires GAGs, we used various GAG perturbants. The small molecule surfen binds to negatively charged GAG species on the cell surface (37). Infection of HapI cells in the presence of surfen led to a 10-fold reduction of MP-12 infection but not vesicular stomatitis virus (VSV) infection (Fig. 3A). Infection of the HapI cells by herpes simplex virus 1 (HSV-1), which is known to utilize heparan sulfate for attachment, was decreased to levels close to background levels by the addition of surfen. Enzymatic removal of cellular heparan sulfate with heparinase also greatly attenuated MP-12 infection (Fig. 3A). Since GAGs are highly negatively charged, nonspecific electrostatic effects could facilitate the interaction between RVFV surface glycoproteins and cellular GAGs. To address this issue, we infected HapI cells in the presence of dextran sulfate, a biologically inert, negatively charged carbohydrate polymer. In contrast to HSV-1, the presence of dextran sulfate had little impact on MP-12 infection (Fig. 3A), suggesting that the interaction with cellular GAGs has some degree of specificity.

Differential requirement for GAGs among *Bunyaviridae* family members. To examine whether the interaction of RVFV with GAGs was unique among bunyaviruses, we infected the *B3GAT3*^{GT} and *B4GALT7*^{GT} cell panels with pathogenic, replication-competent Crimean-Congo hemorrhagic fever virus (CCHFV) and VSV pseudovirions bearing the Andes or Hantaan virus glycoproteins. CCHFV is a member of the *Nairovirus* genus, and both Andes and Hantaan viruses are members of the *Hantavirus* genus, which are further subdivided into New World (Andes virus) and Old World (Hantaan virus) hantaviruses (38, 39). Interestingly, Hantaan virus pseudovirions required catalytically active GlcAT-I and GalT-I for efficient infection of HapI cells, while Andes virus pseudovirions did not (Fig. 3B). Infection with CCHFV was reduced 2-fold when B3GAT3 or B4GALT7 were absent (Fig. 3B). Thus, the role of GAGs during infection by other members of the *Bunyaviridae* family varies.

RVFV utilizes at least one surfen-resistant cellular factor *in vitro*. We next sought to characterize the role of GAGs during MP-12 infection of different cell lines using surfen as an inhibitor of GAG function. We observed that surfen inhibited MP-12 infection in SNB-19 cells, a glioblastoma cell line, but did not inhibit MP-12 infection in HEK 293T or mouse L cells, a mouse epithelium-derived cell line (Fig. 4A), or in Vero cells (data not shown). As a positive control for surfen activity, infection by HSV-1 was strongly inhibited in all cells (Fig. 4A). As an alternative means of examining GAG utilization in L cells, we also tested MP-12 infection in sog9 cells, which are clonal isolates of L cells that are defec-

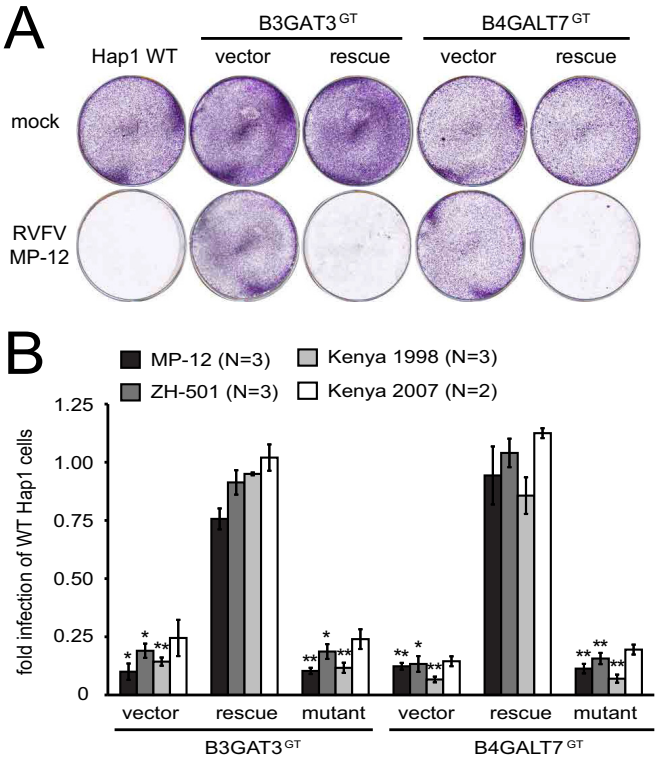

FIG 2 GAGs are important for RVFV infection. (A) Expression of the *B3GAT3* and *B4GALT7* gene products is required for strain MP-12 infection. *B3GAT3* and *B4GALT7* gene-trapped (GT) HapI cells that stably express the empty vector (vector) or wild-type (WT) protein (rescue) were infected with MP-12, and surviving cells were stained with crystal violet. (B) GAGs are important for diverse strains of RVFV. $B3GAT3^{GT}$ and $B4GALT7^{GT}$ HapI cells that stably express the empty vector (vector), the wild-type protein (rescue), or a catalytically inactive point mutant (mutant) were infected with the MP-12, ZH-501, Kenya 980052 (Kenya 1998), and Kenya 2007002444 (Kenya 2007) strains of RVFV, and the percentage of infected cells was normalized to the percentage of infected parental HapI cells. Bars indicate SEMs ($n = 3$ for MP-12, ZH-501, and Kenya 980052; $n = 2$ for Kenya 2007002444). *, $P < 0.005$; **, $P < 0.001$.

tive in the *EXT1* gene (40). EXT1 is responsible for polymerizing disaccharide subunits from the nascent tetrasaccharide linker and was identified in our screen as being important for RVFV infection of HapI cells (Fig. 1B). In contrast to infection by HSV-1, infection by MP-12 was unaffected by the loss of GAGs in sog9 cells (Fig. 4B). To further examine the variance of this GAG-dependent phenotype across cell types, we preincubated RVFV or HSV-1 with either heparin, heparan sulfate, chondroitin sulfate, or dextran sulfate for 1 h prior to infection of a panel of cell lines, including HEK 293T, A549, HeLa, Vero, and (with RVFV only) C6/36 cells, in addition to the HapI cells. Heparin and heparan sulfate inhibited infection of both RVFV and HSV-1 on HEK 293T, A549, HapI, and HeLa cells by at least 2-fold but not on Vero cells, an African green monkey cell line, or of C6/36 cells, an *Aedes albopictus* cell line (Fig. 4C). Similar results were obtained with dextran sulfate, whereas preincubation with chondroitin sulfate had only a very modest effect on the four human cell lines and no effect on the Vero and C6/36 cells (data not shown). Since the composition of GAGs varies between cell types, this suggests that the GAG species that facilitate RVFV infection may not be ubiquitously expressed. Alternatively, as is the case with HSV-1, another entry factor may also be able to compensate for the lack of GAGs on some cell types (41). An endocytosis-mediating receptor(s) for RVFV has not been identified, and these data suggest that multiple entry factors are likely involved in RVFV infection and that their relative importance may vary between cell types.

GAGs are important for RVFV entry and binding. Based on the results of the blocking experiments with surfen and the fact that many viruses utilize GAGs for cellular attachment, we hypothesized that GAGs facilitate efficient entry by enhancing binding of RVFV to HapI cells. To examine this, we took advantage of the VSV pseudovirion system that has been successfully employed for other members of the *Bunyaviridae* family (16). The RVFV surface glycoproteins G_N and G_C are provided in *trans* to replication-incompetent vesicular stomatitis virus lacking its glycoprotein (VSVΔG). To validate the antigenic specificity of RVFV pseudovirions, we pretreated RVFV pseudovirions with an antiserum against RVFV or the severe acute respiratory syndrome (SARS) virus. Infection by RVFV pseudovirions but not those bearing the VSV G protein was inhibited in the presence of the RVFV antisera (Fig. 5A). Infection by RVFV pseudovirions was also sensitive to lysosomotropic agents (data not shown), consistent with the requirement for acidic endosomal pH for infection with RVFV and other members of the *Bunyaviridae* family (42–45). We then infected the $B3GAT3^{GT}$ and $B4GALT7^{GT}$ cell panels with both RVFV and VSV pseudovirions that express red fluorescent protein (RFP). As with replication-competent RVFV, infection with RVFV pseudovirions required catalytically active GlcAT-I and GalT-I (Fig. 5B). In contrast, infection with pseudovirions bearing the VSV G protein was relatively unaffected, thus directly implicating GAGs in RVFV entry.

To measure RVFV virion binding, we employed a quantitative reverse transcription-PCR (qRT-PCR) assay that detects RVFV L gene copies. We first confirmed the linear range of our assay by diluting MP-12 on HapI cells and measuring relative MP-12 binding and found that virus binding increased linearly with virus input over a 3-log-unit range (data not shown). When this assay was applied to the $B3GAT3^{GT}$ and $B4GALT7^{GT}$ cell panels, MP-12 binding strongly correlated with the presence of catalytically active GlcAT-I and GalT-I (Fig. 6). To confirm the role of GAGs in facilitating RVFV binding, we also measured the effect of surfen on RVFV binding. Consistent with its role in infection, surfen also blocked RVFV binding to a similar degree (Fig. 6). Taking these data together, we conclude that the deficiency in RVFV infection in the absence of GAGs is due to a defect at the level of virion attachment.

PTAR1 deficiency attenuates heparan sulfate expression and confers resistance to RVFV infection. HapI cells lacking a functional *PTAR1* (14) were largely resistant to RVFV infection, and this phenotype could be corrected by reintroduction of wild-type *PTAR1* cDNA (Fig. 7A), indicating that the virus resistance phenotype was caused by the loss of PTAR1. In line with previous observations (11, 14), PTAR1-deficient cells showed a marked decrease in cell surface heparan sulfate abundance, as measured by flow cytometry (Fig. 7B). Similar to the virus resistance phenotype, heparan sulfate deficiency, too, could be corrected by complementation with wild-type *PTAR1* cDNA (Fig. 7A and B). Considering the requirement of heparan sulfate for RVFV infection, it seems plausible that improper presentation of heparan sulfate at

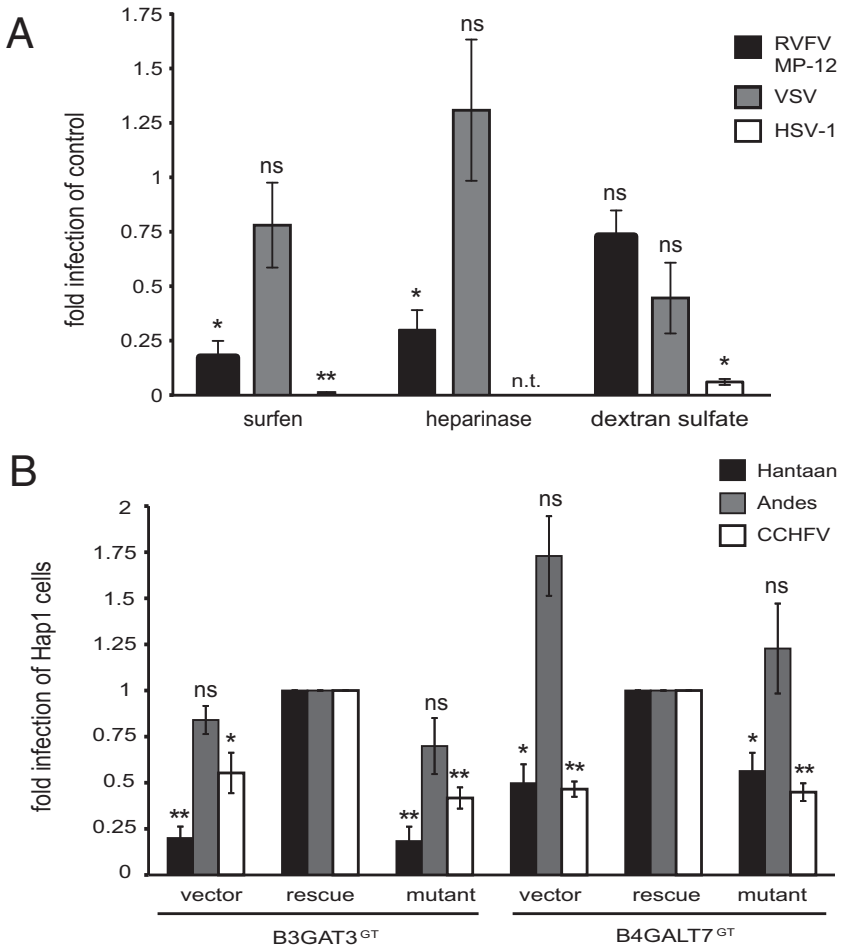

FIG 3 Perturbants of GAGs and the requirement of GAGs among bunyaviruses. (A) GAG perturbants reduce the MP-12 infectivity of HapI cells. HapI cells were pretreated with the small molecule surfen (5 μM), heparinase I (3 U/ml), or dextran sulfate (50 μg/ml) and infected with MP-12, VSV, or HSV-1. The percentage of infected cells was normalized to the percentage of infected cells treated with the vehicle control (dimethyl sulfoxide for surfen, PBS for heparinase I, and water for dextran sulfate). Bars indicate SEMs ($n = 3$). *, $P < 0.005$; **, $P < 0.0001$; ns, no significant difference; n.t., not tested. (B) Role of GAGs for various members of the *Bunyaviridae* family. *B3GAT3*^{GT} and *B4GALT7*^{GT} cells (see Fig. 2 legend) were infected with either Hantaan or Andes virus pseudovirions or replication-competent CCHFV. The percentage of infected cells was normalized to the percentage of infected wild-type cells rescued with each protein. Bars indicate SEMs ($n = 3$). *, $P < 0.05$; **, $P < 0.005$; ns, no significant difference.

the cell surface is responsible for the observed virus resistance of PTAR1-deficient cells. Thus, our screen has identified host factors required for RVFV infection. These factors are involved in various steps of the heparan sulfate biosynthesis pathway and include *PTAR1*, which constitutes a novel RVFV host factor affecting heparan sulfate biogenesis.

DISCUSSION

Cell surface carbohydrates can affect virus entry at the stage of virion attachment, but the importance of this interaction varies among viruses and cells. For example, sialic acid is thought to be sufficient for influenza virus attachment and entry, while the role of GAGs during HSV-1 entry is more complex (41, 46, 47). The herpesviruses are thought to first engage heparan sulfate on the surface of cells before engaging specific receptors (48). Heparan sulfate greatly facilitates HSV-1 attachment and infection under many conditions but is not essential for infection in all contexts (41, 49). For example, CHO cell mutants deficient in GAG synthesis can be rendered permissive by expressing either of the HSV-1 entry receptors nectin-1 (*PVRL1*) or HVEM (*TNFRSF14*) (50). The expression levels of viral receptors can therefore determine whether GAGs are required for efficient viral entry.

The cellular receptor(s) for RVFV is currently not known, and since a nonpermissive cell line is yet to be described, it is possible that more than one molecule may serve as a receptor for RVFV. The C-type lectin DC-SIGN has been shown to promote the binding and internalization of RVFV on dermal dendritic cells, although this protein is not expressed in most of the tissues which the virus has been shown to infect (51). A genome-wide RNA interference screen performed by Hopkins and colleagues did not identify glycosaminoglycans among their list of genes that impacted RVFV infection (52). We have shown that several perturbations of GAGs inhibited RVFV entry and attachment on some cell types, but the relative contribution of other RVFV entry factors remains unknown. Because we observed differential sensitivities of RVFV to surfen, it is possible that the requirement for GAGs across cell types is a

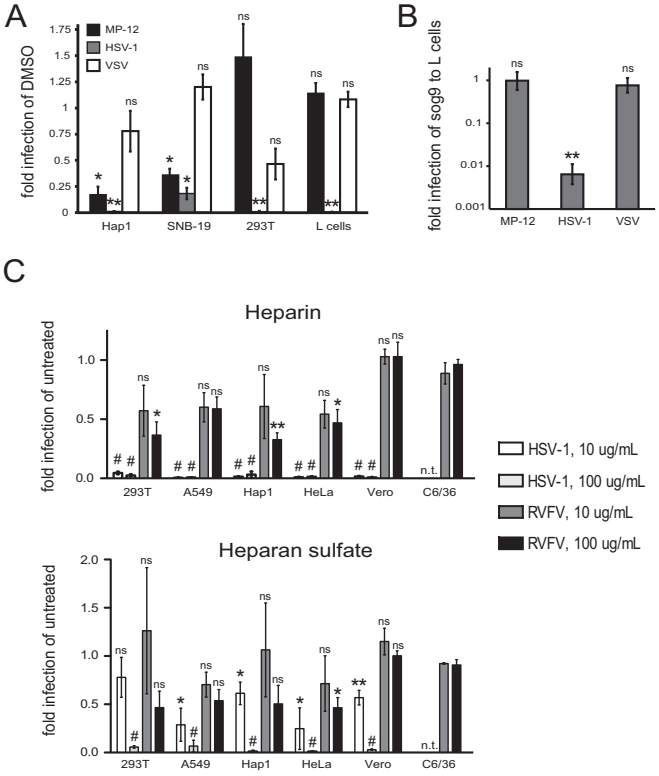

FIG 4 Examination of GAG utilization by MP-12 during infection of various cell lines. (A) MP-12 infection is resistant to surfen in some cell lines. Various cell lines were infected with MP-12, HSV-1, and VSV in the presence of either dimethyl sulfoxide (DMSO) or 5 μM surfen. The percentage of infected cells was normalized to the percentage of infected cells in the dimethyl sulfoxide-treated group. (B) L and sog9 cells were infected with MP-12, HSV-1, and VSV. The percentage of infected sog9 cells was normalized to the percentage of infected L cells. Bars indicate SEMs ($n = 3$). *, $P < 0.01$; **, $P < 0.0001$; ns, no significant difference. (C) Preincubation of HSV-1 or RVFV (MP-12 strain) with either soluble heparin or heparan sulfate prior to infection of HEK 293T, A549, HapI, HeLa, Vero, or C6/36 cells. The concentrations listed to the right of the graphs refer to the concentration of GAG species used during preincubation. Bars indicate SEMs ($n = 3$ for all cells except C6/36 cells, for which $n = 2$). *, $P < 0.05$; **, $P < 0.01$; #, $P < 0.001$; ns, no significant difference.

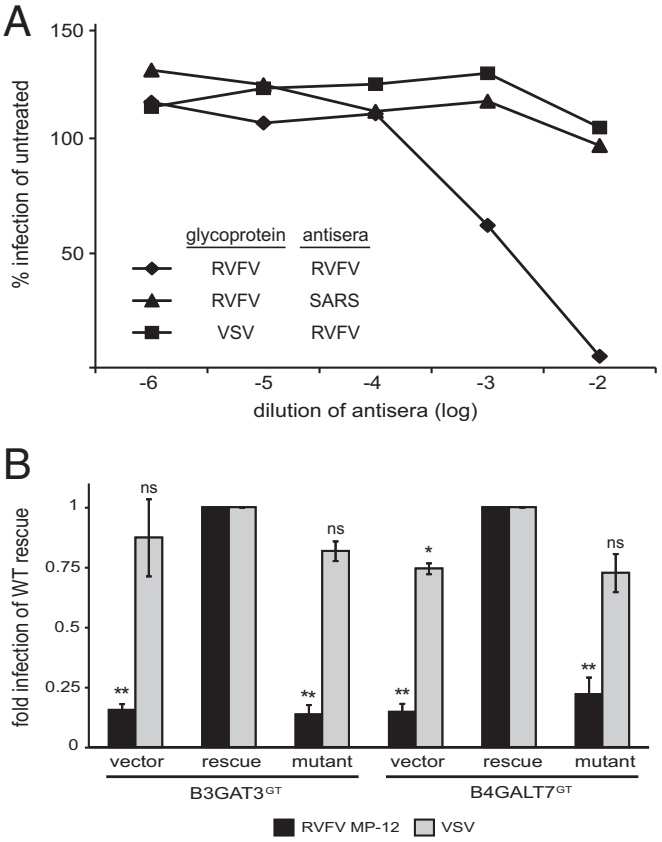

FIG 5 Cellular GAGs are important for RVFV entry. (A) Validation of RVFV pseudovirions. RVFV and VSV pseudovirions were preincubated with antiserum against either RVFV or the SARS virus before infection of Vero E6 cells. Infection values are normalized to the viral inoculum used with untreated cells. (B) *B3GAT3*^{GT} and *B4GALT7*^{GT} HapI cells that stably express the empty vector, the wild-type protein, or a catalytically inactive point mutant were infected with either RVFV or VSV pseudovirions. The percentage of infected cells was normalized to the percentage of infected wild-type cells rescued with each protein. Bars indicate SEMs ($n = 3$). *, $P < 0.01$; **, $P < 0.005$; ns, no significant difference.

function of the relative expression levels of an uncharacterized RVFV receptor(s), GAG structures to which surfen binds inefficiently, or unidentified attachment factors. Indeed, the composition of cellular GAGs between cells is highly variable (53). While heparan sulfate is the best-studied variant, there are at least four other species, each consisting of a unique disaccharide unit. Several enzymes are involved in modifying the different glycan side chains following polymerization. For example, HSV-1 interacts with 3-O-sulfated heparan sulfate, which is catalyzed by the 3-*O*-sulfotransferase family of enzymes (49). Our data suggest that RVFV may require a specific enzymatic variant of a GAG species or cellular proteoglycan. Further work is needed to elucidate the role of specific GAG-modifying enzymes and cellular glycoproteins during RVFV infection.

Heparan sulfate has previously been implicated as playing a role in RVFV infection. A study by de Boer et al. employed a replication-incompetent virus-like particle (VLP) system and found that CHO cells with genetic deficiencies in GAG synthesis were highly resistant, though not immune, to RVFV infection (13). This is in line with our observation that HapI cells incapable of producing GAGs are approximately 10-fold more refractory to RVFV infection than their parental (wild-type) HapI cells. Infection by Toscana virus, another member of the genus *Phlebovirus* of the family *Bunyaviridae*, has been shown to be inhibited by bovine lactoferrin through competition for GAGs on the cell surface (54). These results and our finding that the importance of GAGs and heparan sulfate for RVFV infection exhibited cell type dependence suggest that these molecules serve as virus attachment factors that can enhance but that are not absolutely required for virus infection and therefore do not represent indispensable viral receptors.

By employing RVFV-VSVΔG pseudovirions and an RVFV binding assay, we definitively linked GAGs to RVFV entry and, more specifically, to virus binding. It remains to be determined whether the impact of heparan sulfate on RVFV infection of some cell types reflects the inefficiencies of cell-free virus attachment *in vitro* or whether these interactions are important *in vivo* as well, though the fact that primary RVFV strains behaved similarly to the MP-12 vaccine strain shows that these interactions are not the

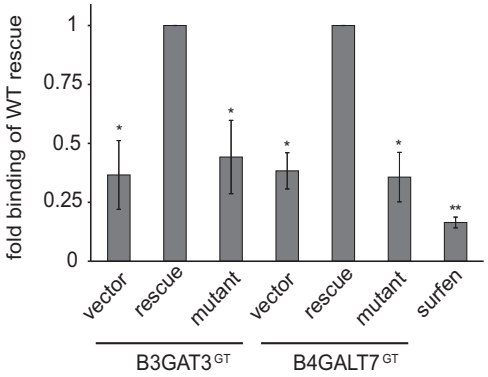

FIG 6 Cellular GAGs are important for RVFV binding. *B3GAT3*^{GT} and *B4GALT7*^{GT} HapI cells that stably express the empty vector, the wild-type protein, or a catalytically inactive point mutant were incubated with MP-12 for 1 h at 37°C, and the amount of cell-associated MP-12 was normalized to the number of wild-type cells rescued with each protein. The amount of cell-associated MP-12 on wild-type HapI cells was also measured in the presence of dimethyl sulfoxide or surfen and normalized to that for dimethyl sulfoxide-treated samples. Bars indicate SEMs ($n = 5$ for HapI gene-trapped mutant cells, $n = 3$ for surfen-treated cells). *, $P < 0.05$; **, $P < 0.001$; ns, no significant difference.

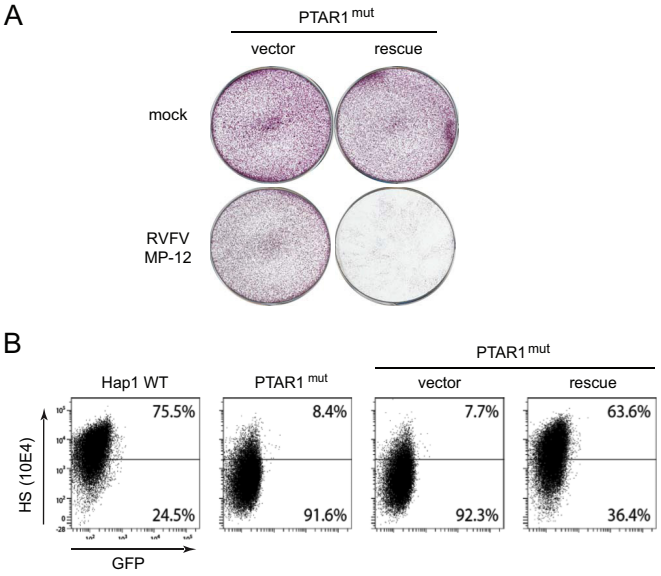

FIG 7 The loss of PTAR1 renders cells resistant to RVFV infection and leads to decreased heparan sulfate levels on the cell surface. (A) Infection of wild-type and PTAR1 mutant (PTAR1^{mut}) cells with MP-12. Surviving cells were visualized by crystal violet staining. (B) Flow cytometric analysis of heparan sulfate (HS) levels, using a specific antibody (10E4), on the surfaces of nonpermeabilized wild-type cells, PTAR1 mutant cells, and PTAR1 mutant cells complemented with either an empty vector or *PTAR1* cDNA. The percentage of cells above and below a signal threshold (horizontal line) is indicated. In line with previous observations (11, 14), the loss of PTAR1 reduces the levels of heparan sulfate present on the cell surface, and these levels can be corrected by introduction of *PTAR1* cDNA.

result of *in vitro* virus adaptation. Interestingly, the tissue tropism of adeno-associated virus 2 (AAV2) to the liver and kidney, organs in which RVFV also establishes productive infection, is exquisitely linked to interactions with GAGs (55–58). Infections with RVFV in pregnant livestock are especially devastating, and pathological studies of infected pregnant livestock reported extremely high virus titers in the placenta, an organ whose cells express high levels of surface GAGs (59, 60). Interactions with placental GAGs may explain the mechanism by which RVFV localizes to the placenta from the bloodstream.

The haploid genetic screen utilized here identified multiple genes involved in GAG synthesis or transport, including *PTAR1*. Whereas we cannot formally exclude the possibility that PTAR1 affects virus susceptibility by other means, it is most likely also involved in mediating GAG-dependent viral entry. Cells deficient for PTAR1 displayed decreased levels of heparan sulfate at their cell surface, which is in agreement with the observations obtained with cells with PTAR1 mutations in previous genetic screens (11, 14). Additional experiments examining the precise role of PTAR1 in heparan sulfate biogenesis and trafficking are needed to shed light on the mechanism of PTAR1-dependent RVFV infection. Finally, the ability of this screening approach to identify additional host factors that are important for RVFV infection may be enhanced by employing cell types where virus attachment occurs in a GAG-independent manner.

The interaction of primary pathogenic RVFV isolates with GAGs suggests that this interaction might be an attractive pharmacological target in humans or other animals. Heparan sulfate has indeed been shown to be important in human papillomavirus infection of mouse female genital tracts (61), and administering anti-heparan sulfate peptides as a prophylactic eye drop was shown to inhibit the spread of HSV-1 in the mouse cornea (62, 63). Although we need to further characterize the exact role of GAGs during RVFV infection *in vitro* and *in vivo*, our current study suggests that disruption of virus-GAG interactions could be a viable antiviral therapy or prophylactic measure.

ACKNOWLEDGMENTS

We thank Stuart Nichol, Nigel Fraser, Jay Gardner, Frank Tufaro, Chuck Whitbeck, Anissa Alexander, Farida Shaheen, and Meda Higa for various reagents and technical assistance.

This work was supported by Cancer Genomics Center (CGC.nl) NWO-VIDI grant 91711316 and a European Research Council (ERC) starting grant (ERC-2012-StG 309634) to T.R.B. and by National Institutes of Health grant U54AI057168 to R.W.D.

FUNDING INFORMATION

This work was funded by HHS | National Institutes of Health (NIH) under grant U54AI057168. EC | European Research Council (ERC) provided funding to Thijn R. Brummelkamp under grant number ERC-2012-StG 309634. Nederlandse Organisatie voor Wetenschappelijk Onderzoek (NWO) provided funding to Thijn R. Brummelkamp under grant number 91711316.

REFERENCES

1. **Schmaljohn CS, Nichol ST.** 2007. Bunyaviridae, p 1741–1789. *In* Knipe DM, Howley PM, Griffin DE, Lamb RA, Martin MA, Roizman B, Straus SE (ed), Fields virology, 5th ed. Lippincott Williams & Wilkins, Philadelphia, PA.
2. **Clements AC, Pfeiffer DU, Martin V, Otte MJ.** 2007. A Rift Valley fever atlas for Africa. Prev Vet Med **82:**72–82. http://dx.doi.org/10.1016/j.prevetmed.2007.05.006.
3. **Madani T, Al-Mazrou YY, Al-Jeffri MH, Mishkhas A, Al-Rabeah AM, Turkistani AM, Al-Sayed MO, Abodahish A, Khan AS, Ksiazek TG, Shobokshi O.** 2003. Rift Valley fever epidemic in Saudi Arabia: epidemiological, clinical, and laboratory characteristics. Clin Infect Dis **37:**1084–1092. http://dx.doi.org/10.1086/378747.
4. **Al-Hazmi M, Ayoola EA, Abdurahman M, Banzal S, Ashraf J, El-Bushra A, Hazmi A, Abdullah M, Abbo H, Elamin A, Al-Sammani E-T, Gadour**

M, Menon C, Hamza M, Rahim I, Hafez M, Jambavalikar M, Arishi H, Aqeel A. 2003. Epidemic Rift Valley fever in Saudi Arabia: a clinical study of severe illness in humans. Clin Infect Dis **36:**245–252. http://dx.doi.org/10.1086/345671.

5. **Daubney R, Hudson JR, Garnham PC.** 1931. Enzootic hepatitis or Rift Valley fever. An undescribed virus disease of sheep cattle and man from East Africa. J Pathol Bacteriol **34:**545–579.
6. **Bird BH, Ksiazek TG, Nichol ST, MacLachlan NJ.** 2009. Rift Valley fever virus. J Am Vet Med Assoc **234:**883–893. http://dx.doi.org/10.2460/javma.234.7.883.
7. **Carette JE, Guimaraes CP, Varadarajan M, Park AS, Wuethrich I, Godarova A, Kotecki M, Cochran BH, Spooner E, Ploegh HL, Brummelkamp TR.** 2009. Haploid genetic screens in human cells identify host factors used by pathogens. Science **326:**1231–1235. http://dx.doi.org/10.1126/science.1178955.
8. **Rosmarin DM, Carette JE, Olive AJ, Starnbach MN, Brummelkamp TR, Ploegh HL.** 2012. Attachment of Chlamydia trachomatis L2 to host cells requires sulfation. Proc Natl Acad Sci U S A **109:**10059–10064. http://dx.doi.org/10.1073/pnas.1120244109.
9. **Carette JE, Guimaraes CP, Wuethrich I, Blomen VA, Sun C, Bell G, Yuan B, Muellner MK, Nijman M, Ploegh HL, Brummelkamp TR.** 2011. Global gene disruption in human cells to assign genes to phenotypes. Nat Biotechnol **29:**542–546. http://dx.doi.org/10.1038/nbt.1857.
10. **Carette JE, Raaben M, Wong AC, Herbert AS, Obernosterer G, Mulherkar N, Kuehne AI, Kranzusch PJ, Griffin AM, Ruthel G, Dal Cin P, Dye JM, Whelan SP, Chandran K, Brummelkamp TR.** 2011. Ebola virus entry requires the cholesterol transporter Niemann-Pick C1. Nature **477:**340–343. http://dx.doi.org/10.1038/nature10348.
11. **Jae LT, Raaben M, Riemersma M, van Beusekom E, Blomen V, Velds A, Kerkhoven RM, Carette JE, Topaloglu H, Meinecke P, Wessels MW, Lefeber DJ, Whelan SP, van Bokhoven H, Brummelkamp TR.** 2013. Deciphering the glycosylome of dystroglycanopathies using haploid screens for Lassa virus entry. Science **340:**479–483. http://dx.doi.org/10.1126/science.1233675.
12. **Jae LT, Raaben M, Herbert AS, Kuehne AI, Wirchnianski AS, Soh TK, Stubbs SH, Janssen H, Damme M, Saftig P, Whelan SP, Dye JM, Brummelkamp TR.** 2014. Lassa virus entry requires a trigger-induced receptor switch. Science **344:**1506–1510. http://dx.doi.org/10.1126/science.1252480.
13. **de Boer SM, Kortekaas J, de Haan CAM, Moormann RJM, Bosch BJ.** 2012. Heparan sulfate facilitates Rift Valley fever virus entry into the cell. J Virol **86:**13767–13771. http://dx.doi.org/10.1128/JVI.01364-12.
14. **Blomen VA, Májek P, Jae LT, Bigenzahn JW, Nieuwenhuis J, Staring J, Sacco R, van Diemen FR, Olk N, Stukalov A, Marceau C, Janssen H, Carette JE, Bennett KL, Colinge J, Superti-Furga G, Brummelkamp TR.** 15 October 2015. Gene essentiality and synthetic lethality in haploid human cells. Science. http://dx.doi.org/10.1126/science.aac7557.
15. **Ray N, Whidby J, Stewart S, Hooper JW, Bertolotti-Ciarlet A.** 2010. Study of Andes virus entry and neutralization using a pseudovirion system. J Virol Methods **163:**416–423. http://dx.doi.org/10.1016/j.jviromet.2009.11.004.
16. **Higa MM, Petersen J, Hooper J, Doms RW.** 2012. Efficient production of Hantaan and Puumala pseudovirions for viral tropism and neutralization studies. Virology **423:**134–142. http://dx.doi.org/10.1016/j.virol.2011.08.012.
17. **Livak KJ, Schmittgen TD.** 2001. Analysis of relative gene expression data using real-time quantitative PCR and the 2(−delta delta C(T)) method. Methods **25:**402–408. http://dx.doi.org/10.1006/meth.2001.1262.
18. **Cuellar K, Chuong H, Hubbell SM, Hinsdale ME.** 2007. Biosynthesis of chondroitin and heparan sulfate in Chinese hamster ovary cells depends on xylosyltransferase II. J Biol Chem **282:**5195–5200. http://dx.doi.org/10.1074/jbc.M611048200.
19. **Pönighaus C, Ambrosius M, Casanova JC, Prante C, Kuhn J, Esko JD, Kleesiek K, Götting C.** 2007. Human xylosyltransferase II is involved in the biosynthesis of the uniform tetrasaccharide linkage region in chondroitin sulfate and heparan sulfate proteoglycans. J Biol Chem **282:**5201–5206. http://dx.doi.org/10.1074/jbc.M611665200.
20. **Casanova JC, Kuhn J, Kleesiek K, Götting C.** 2008. Heterologous expression and biochemical characterization of soluble human xylosyltransferase II. Biochem Biophys Res Commun **365:**678–684. http://dx.doi.org/10.1016/j.bbrc.2007.10.206.
21. **Okajima T, Yoshida K, Kondo T, Furukawa K.** 1999. Human homolog of Caenorhabditis elegans sqv-3 gene is galactosyltransferase I involved in the biosynthesis of the glycosaminoglycan-protein linkage region of proteoglycans. J Biol Chem **274:**22915–22918. http://dx.doi.org/10.1074/jbc.274.33.22915.
22. **Kitagawa H, Tone Y, Tamura J, Neumann KW, Ogawa T, Oka S, Kawasaki T, Sugahara K.** 1998. Molecular cloning and expression of glucuronyltransferase I involved in the biosynthesis of the glycosaminoglycan-protein linkage region of proteoglycans. J Biol Chem **273:**6615–6618. http://dx.doi.org/10.1074/jbc.273.12.6615.
23. **Bai X, Zhou D, Brown JR, Hennet T, Esko JD.** 2001. Biosynthesis of the linkage region of glycosaminoglycans: cloning and activity of galactosyltransferase II, the sixth member of the beta 1,3-galactosyltransferase family (beta 3GalT6). J Biol Chem **276:**48189–48195.
24. **Lind T, Tufaro F, McCormick C, Lindahl U, Lidholt K.** 1998. The putative tumor suppressors EXT1 and EXT2 are glycosyltransferases required for the biosynthesis of heparan sulfate. J Biol Chem **273:**26265–26268. http://dx.doi.org/10.1074/jbc.273.41.26265.
25. **Aikawa J, Grobe K, Tsujimoto M, Esko JD.** 2001. Multiple isozymes of heparan sulfate/heparin GlcNAc N-deacetylase/GlcN N-sulfotransferase. J Biol Chem **276:**5876–5882. http://dx.doi.org/10.1074/jbc.M009606200.
26. **Kamiyama S, Suda T, Ueda R, Suzuki M, Okubo R, Kikuchi N, Chiba Y, Goto S, Toyoda H, Saigo K, Watanabe M, Narimatsu H, Jigami Y, Nishihara S.** 2003. Molecular cloning and identification of 3′-phosphoadenosine 5′-phosphosulfate transporter. J Biol Chem **278:**25958–25963. http://dx.doi.org/10.1074/jbc.M302439200.
27. **Spicer AP, Kaback LA, Smith TJ, Seldin MF.** 1998. Molecular cloning and characterization of the human and mouse UDP-glucose dehydrogenase genes. J Biol Chem **273:**25117–25124. http://dx.doi.org/10.1074/jbc.273.39.25117.
28. **Moriarity JL, Hurt KJ, Resnick AC, Storm PB, Laroy W, Schnaar RL, Snyder SH.** 2002. UDP-glucuronate decarboxylase, a key enzyme in proteoglycan synthesis. J Biol Chem **277:**16968–16975. http://dx.doi.org/10.1074/jbc.M109316200.
29. **Ungar D, Oka T, Brittle EE, Vasile E, Lupashin V, Chatterton JE, Heuser JE, Krieger M, Waters MG.** 2002. Characterization of a mammalian Golgi-localized protein complex, COG, that is required for normal Golgi morphology and function. J Cell Biol **157:**405–415. http://dx.doi.org/10.1083/jcb.200202016.
30. **Kingsley DM, Kozarsky KF, Segal M, Krieger M.** 1986. Three types of low density lipoprotein receptor-deficient mutant have pleiotropic defects in the synthesis of N-linked, O-linked, and lipid-linked carbohydrate chains. J Cell Biol **102:**1576–1585. http://dx.doi.org/10.1083/jcb.102.5.1576.
31. **Eimer S, Gottschalk A, Hengartner M, Horvitz HR, Richmond J, Schafer WR, Bessereau J-L.** 2007. Regulation of nicotinic receptor trafficking by the transmembrane Golgi protein UNC-50. EMBO J **26:**4313–4323. http://dx.doi.org/10.1038/sj.emboj.7601858.
32. **Charng WL, Yamamoto S, Jaiswal M, Bayat V, Xiong B, Zhang K, Sandoval H, David G, Gibbs S, Lu HC, Chen K, Giagtzoglou N, Bellen HJ.** 2014. Drosophila Tempura, a novel protein prenyltransferase α subunit, regulates Notch signaling via Rab1 and Rab11. PLoS Biol **12:**e1001777. http://dx.doi.org/10.1371/journal.pbio.1001777.
33. **Gulberti S, Fournel-Gigleux S, Mulliert G, Aubry A, Netter P, Magdalou J, Ouzzine M.** 2003. The functional glycosyltransferase signature sequence of the human beta 1,3-glucuronosyltransferase is a XDD motif. J Biol Chem **278:**32219–32226. http://dx.doi.org/10.1074/jbc.M207899200.
34. **Byrnes AP, Griffin DE.** 2000. Large-plaque mutants of Sindbis virus show reduced binding to heparan sulfate, heightened viremia, and slower clearance from the circulation. J Virol **74:**644–651. http://dx.doi.org/10.1128/JVI.74.2.644-651.2000.
35. **Sugahara Y, Matsumura T, Kono Y, Honda E, Kida H, Okazaki K.** 1997. Adaptation of equine herpesvirus 1 to unnatural host led to mutation of the gC resulting in increased susceptibility of the virus to heparin. Arch Virol **142:**1849–1856. http://dx.doi.org/10.1007/s007050050202.
36. **Sa-Carvalho D, Rieder E, Baxt B, Rodarte R, Tanuri A, Mason PW.** 1997. Tissue culture adaptation of foot-and-mouth disease virus selects viruses that bind to heparin and are attenuated in cattle. J Virol **71:**5115–5123.
37. **Schuksz M, Fuster MM, Brown JR, Crawford BE, Ditto DP, Lawrence R, Glass C, Wang L, Tor Y, Esko JD.** 2008. Surfen, a small molecule antagonist of heparan sulfate. Proc Natl Acad Sci U S A **105:**13075–13080. http://dx.doi.org/10.1073/pnas.0805862105.
38. **Bente DA, Forrester NL, Watts DM, McAuley AJ, Whitehouse CA, Bray M.** 2013. Crimean-Congo hemorrhagic fever: history, epidemiology,

pathogenesis, clinical syndrome and genetic diversity. Antiviral Res **100:** 159–189. http://dx.doi.org/10.1016/j.antiviral.2013.07.006.
39. **Mir MA.** 2010. Hantaviruses. Clin Lab Med **30:**67–91. http://dx.doi.org/10.1016/j.cll.2010.01.004.
40. **Banfield BW, Leduc Y, Esford L, Schubert K, Tufaro F.** 1995. Sequential isolation of proteoglycan synthesis mutants by using herpes simplex virus as a selective agent: evidence for a proteoglycan-independent virus entry pathway. J Virol **69:**3290–3298.
41. **Bender FC, Whitbeck JC, Lou H, Gary H, Eisenberg RJ, Cohen GH.** 2005. Herpes simplex virus glycoprotein B binds to cell surfaces independently of heparan sulfate and blocks virus entry. J Virol **79:**11588–11597. http://dx.doi.org/10.1128/JVI.79.18.11588-11597.2005.
42. **Lozach P-Y, Mancini R, Bitto D, Meier R, Oestereich L, Overby AK, Pettersson RF, Helenius A.** 2010. Entry of bunyaviruses into mammalian cells. Cell Host Microbe **7:**488–499. http://dx.doi.org/10.1016/j.chom.2010.05.007.
43. **Filone CM, Heise M, Doms RW, Bertolotti-Ciarlet A.** 2006. Development and characterization of a Rift Valley fever virus cell-cell fusion assay using alphavirus replicon vectors. Virology **356:**155–164. http://dx.doi.org/10.1016/j.virol.2006.07.035.
44. **Plassmeyer ML, Soldan SS, Stachelek KM, Martín-García J, González-Scarano F.** 2005. California serogroup Gc (G1) glycoprotein is the principal determinant of pH-dependent cell fusion and entry. Virology **338:** 121–132. http://dx.doi.org/10.1016/j.virol.2005.04.026.
45. **Hofmann H, Li X, Zhang X, Liu W, Kühl A, Kaup F, Soldan SS, González-Scarano F, Weber F, He Y, Pöhlmann S.** 2013. Severe fever with thrombocytopenia virus glycoproteins are targeted by neutralizing antibodies and can use DC-SIGN as a receptor for pH-dependent entry into human and animal cell lines. J Virol **87:**4384–4394. http://dx.doi.org/10.1128/JVI.02628-12.
46. **Tiwari V, O'Donnell C, Copeland RJ, Scarlett T, Liu J, Shukla D.** 2007. Soluble 3-O-sulfated heparan sulfate can trigger herpes simplex virus type 1 entry into resistant Chinese hamster ovary (CHO-K1) cells. J Gen Virol **88:**1075–1079. http://dx.doi.org/10.1099/vir.0.82476-0.
47. **Choudhary S, Marquez M, Alencastro F, Spors F, Zhao Y, Tiwari V.** 2011. Herpes simplex virus type-1 (HSV-1) entry into human mesenchymal stem cells is heavily dependent on heparan sulfate. J Biomed Biotechnol **2011:**264350. http://dx.doi.org/10.1155/2011/264350.
48. **Spear PG.** 2004. Herpes simplex virus: receptors and ligands for cell entry. Cell Microbiol **6:**401–410. http://dx.doi.org/10.1111/j.1462-5822.2004.00389.x.
49. **Shukla D, Liu J, Blaiklock P, Shworak NW, Bai X, Esko JD, Cohen GH, Eisenberg RJ, Rosenberg RD, Spear PG.** 1999. A novel role for 3-O-sulfated heparan sulfate in herpes simplex virus 1 entry. Cell **99:**13–22. http://dx.doi.org/10.1016/S0092-8674(00)80058-6.
50. **Tsvitov M, Frampton AR, Shah WA, Wendell SK, Ozuer A, Kapacee Z, Goins WF, Cohen JB, Glorioso JC.** 2007. Characterization of soluble glycoprotein D-mediated herpes simplex virus type 1 infection. Virology **360:**477–491. http://dx.doi.org/10.1016/j.virol.2006.10.039.
51. **Lozach P-Y, Kühbacher A, Meier R, Mancini R, Bitto D, Bouloy M, Helenius A.** 2011. DC-SIGN as a receptor for phleboviruses. Cell Host Microbe **10:**75–88. http://dx.doi.org/10.1016/j.chom.2011.06.007.
52. **Hopkins KC, McLane LM, Maqbool T, Panda D, Gordesky-Gold B, Cherry S.** 2013. A genome-wide RNAi screen reveals that mRNA decapping restricts bunyaviral replication by limiting the pools of dcp2-accessible targets for cap-snatching. Genes Dev **27:**1511–1525. http://dx.doi.org/10.1101/gad.215384.113.
53. **Esko JD, Kimata K, Lindahl U.** 2009. Proteoglycans and sulfated glycosaminoglycans. *In* Varki A, Cummings RD, Esko JD, Freeze HH, Stanley S, Bertozzi CR, Hart GW, Etzler ME (ed), Essentials of glycobiology, 2nd ed. Cold Spring Harbor Laboratory Press, Cold Spring Harbor, NY.
54. **Pietrantoni A, Fortuna C, Remoli ME, Ciufolini MG, Superti F.** 2015. Bovine lactoferrin inhibits Toscana virus infection by binding to heparan sulphate. Viruses **7:**480–495. http://dx.doi.org/10.3390/v7020480.
55. **Ikegami T, Makino S.** 2011. The pathogenesis of Rift Valley fever. Viruses **3:**493–519. http://dx.doi.org/10.3390/v3050493.
56. **Summerford C, Samulski RJ.** 1998. Membrane-associated heparan sulfate proteoglycan is a receptor for adeno-associated virus type 2 virions. J Virol **72:**1438–1445.
57. **Gao G, Vandenberghe LH, Alvira MR, Lu Y, Calcedo R, Zhou X, Wilson JM.** 2004. Clades of adeno-associated viruses are widely disseminated in human tissues. J Virol **78:**6381–6388. http://dx.doi.org/10.1128/JVI.78.12.6381-6388.2004.
58. **Zhang F, Aguilera J, Beaudet JM, Xie Q, Lerch TF, Davulcu O, Colón W, Chapman MS, Linhardt RJ.** 2013. Characterization of interactions between heparin/glycosaminoglycan and adeno-associated virus. Biochemistry **52:**6275–6285. http://dx.doi.org/10.1021/bi4008676.
59. **Parmley RT, Takagi M, Denys FR.** 1984. Ultrastructural localization of glycosaminoglycans in human term placenta. Anat Rec **210:**477–484. http://dx.doi.org/10.1002/ar.1092100308.
60. **Gerdes GH.** 2002. Rift Valley fever. Vet Clin North Am Food Anim Pract **18:**549–555. http://dx.doi.org/10.1016/S0749-0720(02)00029-4.
61. **Johnson KM, Kines RC, Roberts JN, Lowy DR, Schiller JT, Day PM.** 2009. Role of heparan sulfate in attachment to and infection of the murine female genital tract by human papillomavirus. J Virol **83:**2067–2074. http://dx.doi.org/10.1128/JVI.02190-08.
62. **Park PJ, Antoine TE, Farooq A, Valyi-Nagy T, Shukla D.** 2013. An investigative peptide-acyclovir combination to control herpes simplex virus type 1 ocular infection. Invest Ophthalmol Vis Sci **54:**6373–6381. http://dx.doi.org/10.1167/iovs.13-12832.
63. **Tiwari V, Liu J, Valyi-Nagy T, Shukla D.** 2011. Anti-heparan sulfate peptides that block herpes simplex virus infection in vivo. J Biol Chem **286:**25406–25415. http://dx.doi.org/10.1074/jbc.M110.201103.